Multi-Disciplinary Analysis and Design Optimization of a 3D Model Airplane

Ruben A. Fernandez[1,2] and Hernando Lugo[1,2]
Florida International University, MAIDROC Lab., Miami, FL 33174, USA

Walid Esiel[2] and Clara Bahoya[2]
Florida International University, Miami, Florida, 33012, USA

The SAE Regular Class Aero Design Competition requires students to design a model scale aircraft with limits to the power consumption, take-off distance, and wingspan, while maximizing the amount of payload it can carry. As a result, the aircraft should be designed subject to these simultaneous and contradicting objectives: 1) minimize the drag, 2) minimize the pitching moment, and 3) maximize the lift. This study aims to determine five optimized geometric design variables: 1) incidence angle of the wing, 2) incidence angle of the horizontal tail, 3) distance between the wing and the tail, 4) sweep angle of the winglets, and 5) height of the winglets. To determine the incidence angles, an airplane was initially designed using the highly cambered S1223 airfoil for the wing and the inverted NACA2409 airfoil for the tail. The same fuselage shape was used for all configurations where the only changes were the incidence angles and the distance between the wing and tail. Wing incidence angle was varied in the range 0° to 10°. Tail incidence angle was varied in the range -5° to 0°. Horizontal distance between the wing and the horizontal tail was varied in the range 4L to 10L, where L is the wing chord length. Each random combination of the design variables defined its own 3D aircraft configuration. Aerodynamics of each of these 3D aircraft shapes including their coefficients of lift, drag, and pitching moment were calculated using ANSYS Fluent software. Fourty such aircraft configurations were analyzed before the results were inputted into modeFrontier software to perform the multi-objective optimization study resulting in a Pareto-optimized set of the best trade-off 3D airplane geometries having the best combination of incidence angles and the wing-tail distance to achieve the three stated goals. Structural 3D analysis and static and dynamic stability analyses were also performed.

I. Nomenclature

Cl	=	coefficient of lift
Cd	=	coefficient of drag
Cm	=	coefficient of pitching moment
C	=	chord length
V	=	speed
L	=	aileron length
S1	=	aileron max deflection
S2	=	servo max deflection
u	=	*X component of local velocity*
v	=	Y component of local velocity
B	=	wingspan
λ	=	taper ration

[1] Undergraduate mechanical engineering student, Department of Mechanical and Materials Eng., MAIDROC Lab.
[2] Undergraduate mechanical engineering student, Department of Mechanical and Materials Eng.

II. Introduction

A. System Overview

The Florida International University (FIU) team designed the Panther Air Cargo-5 (PAC-5) around the payload and mission parameters. PAC-5 will carry one inflated soccer ball and 20 lbf of steel while having a 71-inch wingspan and an 8.6-inch cargo length to achieve a flight score or 104.02. A rectangular wing planform, using the S1223 airfoil, in combination with a conventional tail using the NACA 0009 airfoil for the vertical stabilizer and an inverted NACA2412 airfoil for the horizontal tail will be used in PAC-5 as shown in Figure 1. PAC-5 will also utilize winglets to reduce induced drag during takeoff and flight. This configuration facilitates the flight experience of the pilot, while reducing the complexity of manufacturing. The steel payload will surround the soccer ball without increasing the cargo bay length as shown in Figure 1. A conventional landing gear will be used with inflatable wheels to reduce rolling friction. Loaded PAC-5 aims to take off within 90 feet when powered by a Cobra C4130-20 [1,2] electric motor that produces approximately 12 lbf of thrust with a 20x8e propeller.

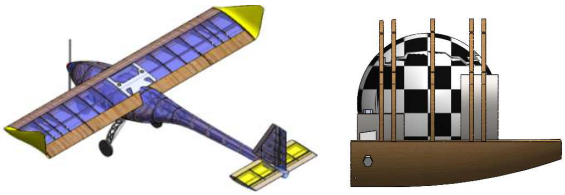

Fig. 1 Isometric view of the PAC-5 airplane and a side view of its cargo bay.

B. Understanding Risk

Throughout the design of the aircraft, several risks had to be taken to potentially achieve the highest score possible. The plane was designed with an increased structural support, oversized control surfaces, and a takeoff distance of 90 ft to increase reliability. As a result, this reduces the overall payload the aircraft can carry. However, this will allow PAC-5 to have various successful flights to maximize the predicted payload bonus and increase the overall flight score. Weather was also taken into consideration during this design project [3].

C. Discriminators

PAC-5 will utilize fully integrated winglets to reduce the induced drag created by a low aspect ratio wing instead of just end plates as various teams utilized last year. The computational fluid dynamics (CFD) results found that the winglets decreased the drag by 9.75% and increased the lift by 5.03%. Getting the idea from the military cargo planes, PAC-5 will have a detachable nose, which will allow us to quickly have access to the payload when unloading. PAC-5 will also have a cargo length limited to the diameter of one soccer ball to increase our score. Our team opted to create and design the landing gear instead of buying a generic one in attempt to save weight.

III.Design Layout & Trades

A. Overall Design Layout and Size

To develop the overall layout of the aircraft, a focus was placed on shrink wrapping the aircraft around the payload and necessary components, while ensuring ease of access as a priority. The wing longitudinal placement is driven by the desired center of gravity (CG) and a 5-15% stability margin achieved through weight data/predictions for each component. Ideal layouts were sketched and then modeled to determine the viability of the idea and enough spacing to accommodate structure. The pros and cons were weighed for other system configurations / layouts [4,5] For

example, pusher *vs.* puller propulsion system, to reach a decision on which would be the most beneficial for the mission and performance. Three conceptual designs were created at the beginning of the design process (Figure 2.)

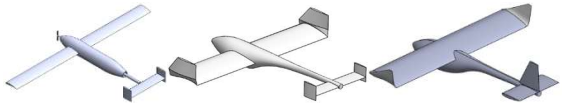

Fig. 2 Conceptual designs C1, C2, & C3.

The C1 concept used a long rectangular wing, an H-Tail, and a conventional fuselage. This design aims to carry about 25 lbm of steel with 4 soccer balls. This configuration was able to carry the most weight and the most soccer balls, but we realized that carrying multiple soccer balls results in a lower score because the cargo length greatly increases. When coupled with a wingspan of 119", this configuration achieves a score of 86.832. Both the C2 and C3 concepts have a wingspan of 71" and aim to carry 1 soccer ball with 20 lbm of steel. Since only one soccer ball was going to be carried, the fuselage was tapered to reduce drag. Both concepts achieve a score of 104.02. The main difference between C2 and C3 is the tail configuration and wing placement. C2 used an H-tail, while C3 uses a conventional tail to reduce the weight of the tail slightly. Lastly, C2 used a mid-wing which created difficulties when integrating the wing and payload. As a result, the wing was shifted up to create a high wing allowing for more space to store the payload. These decisions resulted in concept C3 as the chosen final design. A tricycle landing gear was chosen over that of the tail dragger since it requires a heavy tail structure. A rear gear height of 7.75" and a front gear height of 9.675" was used to provide a 2" vertical clearance for the propeller.

B. Aerodynamic Shape Multi-Objective Optimization of the 3D Airplane

With C3 selected as the design for PAC-5, a multi-objective aerodynamic optimization was conducted taking into account the incidence angle for the wing and horizontal stabilizer, the wing-to-tail distance, height of the winglets, and sweep angle of the winglets. In this study we maximized the lift, while minimizing the drag and moment. Halton's and Sobol's algorithms [6] were utilized to generate 40 random geometries of the complete C3 concept airplane. ANSYS-Fluent CFD software [7] was used to predict the three high fidelity objectives that were used to create the response surfaces for five-dimensional spaces that were then used for optimization of the five design variables. ModeFrontier optimization software [8] was then used to find the Pareto-optimum set (Figure 3) of the five geometric design parameters. The resulting optimum geometry that was chosen provided a 5.03% increase in lift, a 9.75% decrease in drag, and a 40.88% decrease in the pitching moment for PAC-5 aircraft.

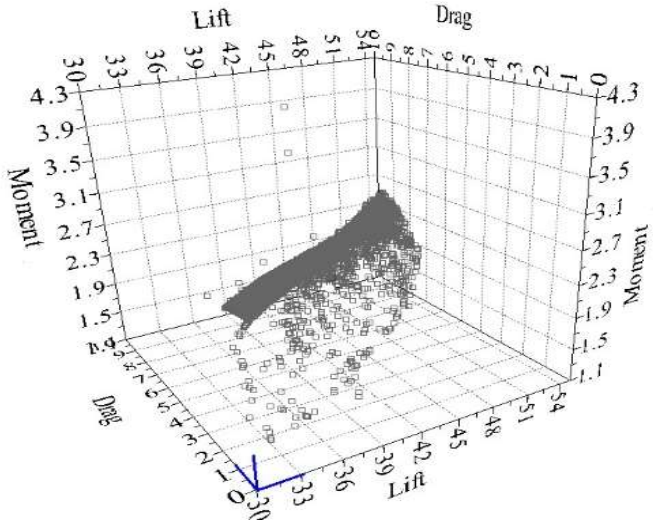

Fig. 3 Pareto frontier of the best trade-off solutions for the 3D optimized airplane configurations.

C. Optimization and Sensitivity Analysis

Careful attention was given to weight savings for the structure of the plane. This resulted in the tail being changed from an H-tail configuration to a conventional tail. This allowed for a 12.5% weight reduction for the tail by simplifying its attachment method. Hexagonal weight saving holes were also added to the wing ribs to reduce weight along with reducing the size of several 3D printed parts such as the wing box and the tail mount. These changes resulted in a total weight reduction of 0.785 lbm. The fuselage had a teardrop shape rather than a conventional cylindrical fuselage shape to help reduce the overall drag. To further minimize drag, winglets were added to help reduce the high induced drag present in rectangular wings especially during takeoff. Implementing the winglets allowed for a 9.75% reduction in drag and an 5.03% increase in lift by maximizing the effective wing area. The position of the tail was also determined by the downwash of the wing. By placing the tail higher up, it was positioned away from the wing downwash in clean undisturbed air.

D. Design Features and Details

The wing will be manufactured using ribs and spars with 15 ribs and 2 load bearing spars as shown in Figure 4. The center rib will be a large 9.375” wide 3D printed section that will also serve as a wing box to attach the wing to the fuselage structure. Each additional rib will have a thickness of 1/8th of an inch with a majority being made of balsa wood, except for the 2 outer ribs and the 2 ribs that will hold the servos which will be laser cut out of lite-ply. This allows for these ribs to withstand expected additional loads. Both spars will be wooden I-beams that were sized to improve the 2nd moment of inertia. The forward spar will be 0.375” by 0.3” and the rear spar will be 0.25” by 0.5”. They will be located at 20.7% and 57.8% of the wing chord length, respectively.

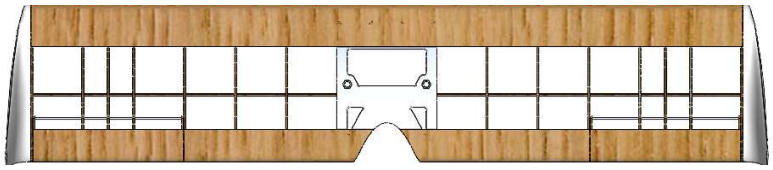

Fig. 4 Top View of the wing

Similarly, the horizontal stabilizer will be composed of 6 ribs and 2 box spars as shown in Figure 5. The forward box spar is located at 19.4% of the chord length, while the rear spar is located at 53.8% of the horizontal tail chord length. A 1/8-inch thick aileron spar will also be added, while 1/32 inch thick stringers will be added in the leading and trailing edge of the elevator. The vertical stabilizer will be composed of 6 ribs and will use 2 rectangular box spars as seen in Figure 5. Both spars will be 0.45” by 0.125” with the forward spar located at 29.6% and the rear spar at 68.8% of the chord length. The positions of the spars were adjusted to allow them to be integrated into the tail mount using two pins.1/32-inch stringers will also be used in the trailing and leading edges of the vertical stabilizer.

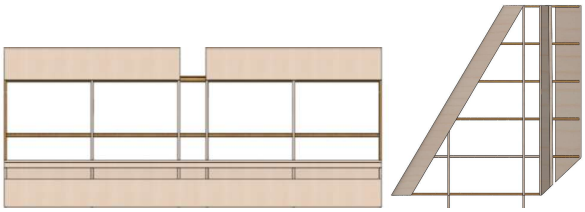

Fig. 5 Horizontal and vertical tails.

The fuselage will be composed of 18 cross sections made of lite-ply and balsa wood with a main load boom located towards the top of the fuselage and an additional load spar at the bottom of the fuselage (Figure 6). Stringers will also be placed on the sides to maintain the shape of the fuselage. A base plate will be located under the payload bay to support the steel and soccer ball.

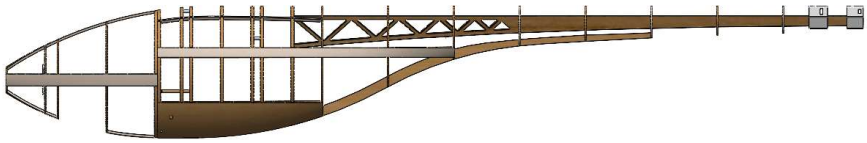

Fig. 6 Side view of the fuselage.

When it came to the design of the landing gear, we evaluated two configurations: tail dragger and tricycle. Both configurations have their own pros and cons, the tricycle configuration was the most beneficial design that met all the requirements. Figure 7 shows the final design of the landing gear using aluminum 7075-T6 satisfying all the recommended angles [9]. The front landing gear is located under the nose of the fuselage where it is attached by two locking nuts preventing vertical motion in addition to two 3D printed supports to prevent lateral motion.

Fig. 7 Isometric view of the landing gear.

IV.Loads and Environments, Assumptions

When designing the landing gear, the focus in mind was to create a design that is light weight and able to withstand a harsh landing, which we simulated to be three times the weight of the aircraft. An important aspect in achieving this goal is choosing the material that the landing gear will be made of. We chose aluminum alloy 7075-T6 since it had both a high yield strength and a relatively low density, which are 73.244 ksi and 165.254 lbm/ft3, respectively. Structural analysis of the landing gear was performed using ANSYS Static Structural. However, the material that we used in the simulation was an aluminum alloy and we had to change the characteristic of the metal to match that of the 7075-T6. We did two separate analyses for the landing gear as it was two separate parts and we wanted to see how each part would react independently of each other. In both simulations, the mesh size used was 0.039” for the bodies. Shown in Fig 8 are the maximum stresses experienced in the front and rear landing gears under 3g conditions, which were 6.7929 ksi and 24.871 ksi, respectively, thus, giving the plane’s landing gear a safety factor of 10.784 for the front landing gear and 2.945 for the rear.

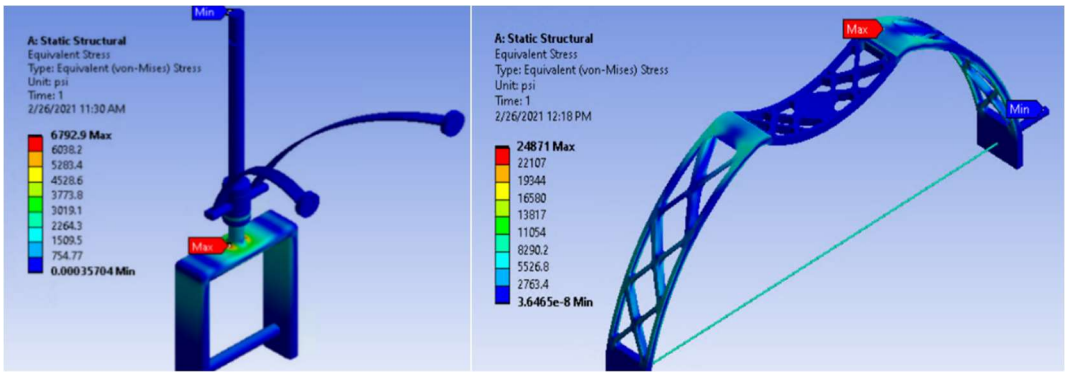

Fig. 8 Static structural simulation of the landing gear.

The team analyzed influence of aerodynamic forces of the plane during flight by completing Finite Element Analysis (FEA) of the main wing structure. We tested the wing structure by applying an upward pressure force of 30 lbf to the main spars on the surface of the wing. To calculate the stress and deformation, we considered the center connection as a fixed support and applied gravity and pressure on the wing. Figure 9 demonstrates a maximum equivalent stress of 2.671 ksi which resulted in 1.639 inches of bending deflection at the wing tips.

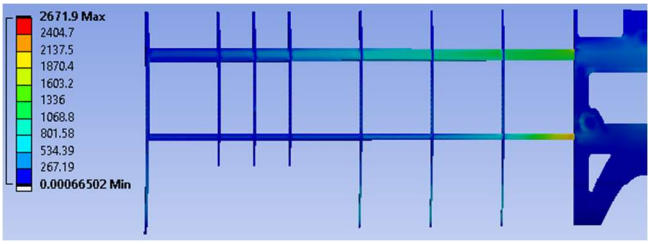

Fig. 9 Static structural simulation of the wing.

The team also applied the maximum lift that will be expected and distributed it using Schrenk's approximate method [4]. This lift distribution was used to develop the internal shear and bending forces that can be expected along the wing's half span as shown in Fig 10. A detailed calculation of the Schrenk's approximation method was performed.

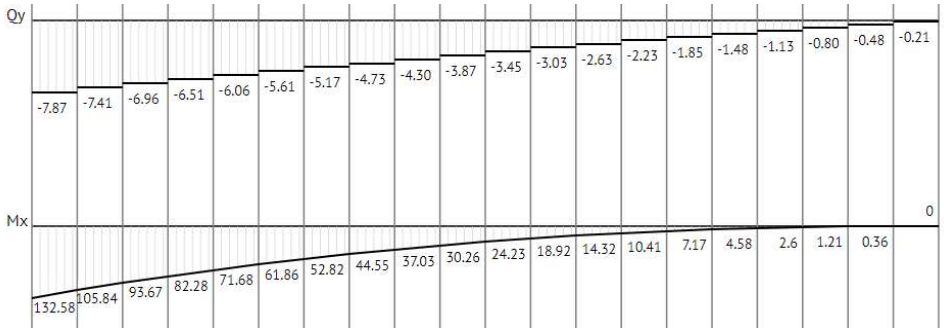

Fig. 10 Shear and bending moment diagram for the wing.

An additional analysis was conducted on the fuselage of the plane to determine how it would hold against the landing that was expected of three times the weight. These results can be seen in Fig 11 where the max stress on the fuselage is 0.533 ksi with a deformation of 0.004". The fuselage was designed to be made of lite-ply which has a yield strength of 5 ksi giving a factor of safety of 9.381 for the fuselage during landing.

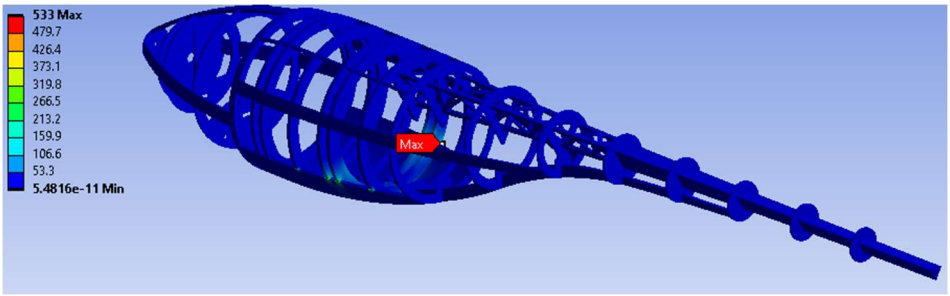

Fig. 11 Fuselage stresses due to landing gear loading.

Finally, structural analyses were performed to test the effects the wing and tail aerodynamic loading would have on the fuselage. Both tail and wing loadings were simulated together as they will always occur simultaneously. The tail downforce was applied at the end of the fuselage boom, while the wing load was applied at the connection points

resulting in a max stress of 2.838 ksi and a deflection of 0.363", corresponding to a factor of safety of 1.762 for the fuselage.

V.Analysis

E. Analysis Tools

The team used multiple software for the design such as, XFLR5, SolidWorks, Ansys, MATLAB, ModeFrontier, MotoCalc, DraftSight, and E300. XFLR5 is an analysis tool for airfoils, wings, and planes operating at low Reynolds number and was crucial for comparative and performance analysis. SolidWorks was utilized to generate the 3D model, drawing, geometric analysis (identifying packaging layout) and weight analysis. MATLAB was used to derive the loads acting on the wing that were applied in ANSYS Static Structural, and to obtain variables for the takeoff simulation Python script. Ansys Static Structural is a finite element analysis software that allows analysis of anisotropic materials. MotoCalc was used for performance predictions for the propulsion system (both static and dynamic). Lastly, E300, provided by Professor Sobieczky [10,11], is a 3D geometry generation code that was utilized to generate various winglet shapes until the desired shape was obtained.

F. Developed Models

For the CFD analysis, PAC-5 SolidWorks was used to create the geometry and ANSYS Fluent was used to generate the computational mesh and run the analysis. The flow domain was a cylinder 57.415 ft long and a radius of 32.808 ft. The inlet located 6.562 ft. from the nose of the plane, was defined as an inlet velocity of 33 mph while the outlet was defined as a pressure outlet. The outer surface of the cylinder was defined with a symmetry boundary condition. A fine grid of 27 million tetrahedron cells was generated to run CFD using Navier Stokes equations with K-Omega SST as the turbulence model. The grid convergence study was performed where CFD results were obtained on 17.5 million, 27 million and 31 million grid cells. A 0.5% change was found after 27 million elements and a finer grid was producing errors due to a lack of computing resources. As a result, 27 million elements were used for all CFD simulations.

G. Runway & Landing Performance

The biggest constraint we had to overcome was the limited runway distance we are given, 100 ft. Getting up to the necessary speed to produce enough lift to carry our payload within the 100 ft proved to be a very challenging task. At full capacity the plane will need to produce around 27.5 lbf. In order to maximize the lift produced by the plane various airfoils were analyzed including the NACA4412, S1223, and E423. Since the S1223 produced the by far the highest lift it was chosen in order to reduce the takeoff velocity. Conducting a CFD simulation on ANSYS Fluent, it was found that a speed of 33 mph was required to achieve takeoff and determined the total drag [5]. Various motors and propeller combinations were then tested to determine the net force and acceleration acting on the plane. Through this calculation it was determined that at least 11 lbf of thrust were required to reach this speed in under 100 feet. Out of all the motors tested the Cobra C4130-20 was the only motor capable of achieving this thrust without exceeding 1000W when paired with a 20x8e propeller. Table 1 shows several motor and propeller combinations that were considered and the max velocity and lift they would be able to produce.

Table 1 Motor and propeller combinations take-off analysis

Prop/ Motor	Cobra C4130-16/16x8e	Cobra C4130-16/15x10e	Cobra C4130-20/20x10e	Cobra C4130-20/20x8e	Cobra C4130-14/15x6e	Hacker A50-14L/20x8e
Thrust (N)	42.1497	36.1084388	53.25019366	49.48368516	43.22837354	51.15455
Watt (W) Input	981	918	921.7	829.5	916	???
Net Force (N)	34.04664	28.0053788	45.14713366	41.38062516	35.12531354	43.05149
Accelration (m/s^2)	2.780949013	2.287495346	3.68764368	3.379993113	2.869055684	3.516470308
Max Takeoff Velocity (m/s)	13.02024008	11.80871357	14.99329046	14.35424607	13.22488694	14.64117584
Max Lift (N)	93.00985243	76.50611483	123.3345857	113.0451005	95.95661212	117.60963

The main advantages of a tricycle configuration are its ease of steering and increase in acceleration at takeoff since the motor and propeller are parallel to the ground. Maintaining the fuselage parallel to the ground also reduces drag

dramatically when compared to a tail dragger configuration. Another advantage from using a tricycle configuration is that when we place the rear wheels close enough to the CG, the moment needed in order to lift the plane will be very low and will allow for the plane to pitch-rotate faster. Another aspect of the landing gear that plays a big role is the wheel selection. The size of wheels affects the acceleration and top speed of the aircraft while on the runway. As the size increases, so does acceleration while top speed decreases. We decided on 4-inch diameter wheels as it gave a favorable balance of acceleration vs. top speed.

H. Flight and Maneuver Performance

Wing sizing was based mainly on the scoring equation to minimize the wingspan and maximizing the payload. With a wingspan of 71" and an aspect ratio of 4.762, PAC-5 airplane will have a wing surface area of 1030 in2 to carry 20 lbm of steel. The horizontal and vertical stabilizers were then initially sized using the tail volume coefficient method and later optimized using XFLR5 and ANSYS Fluent to analyze the full geometry and make small changes to reduce coefficient of moment and drag. The tail will have an arm length of 49.67" with a horizontal tail surface area of 170 in2 and a vertical tail surface area of 85.250 in2. Control surfaces for the wing and tail were sized using the graph, shown in Fig 12 [5], while trying to keep the chord length of the ailerons between 15-25% of the wing chord length and between 25-50% of the tail chord length for the wing and tail, respectively.

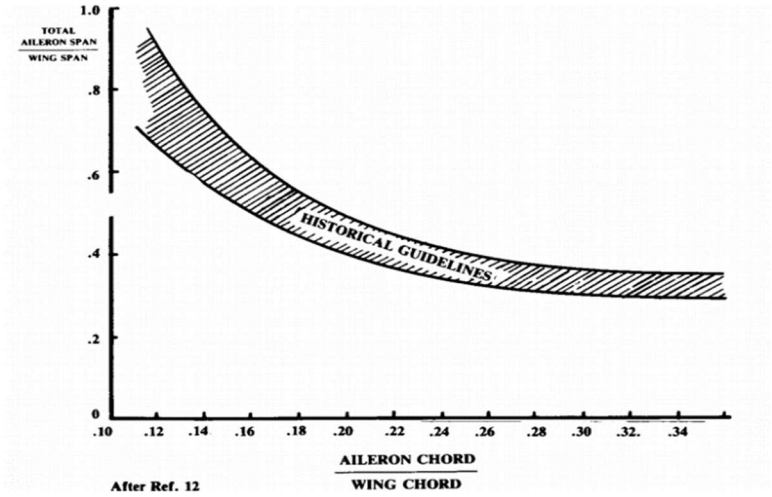

Fig. 12 Wing and tail sizing graph.

Servos were then sized using Equation 1 shown below [5].

$$Torque\ (oz-in) = 8.5^{-6} \times \frac{C^2 \times V^2 \times L \times \sin(S1) \times \tan(S2)}{\tan(S2)} \quad (1)$$

Here, C (in) is the chord length of the aileron, V (mph) is the flight speed, L (in) is the length of the aileron, S1 is the max deflection of the aileron, and S2 is the max deflection of the servo. While the expected average flight speed is about 35 mph, we will use a conservative 45 mph along with a maximum deflection angle of 45 degrees to ensure that our ailerons are adequately sized. Table 2 shows the required torque for each of the control surfaces and the torque rating of the servo that will be used.

Table 2 Servo torque ratings

	Chord (in)	Length (in)	Required Torque (oz - in)	Servo Rated Torque (oz-in)
Aileron	4.25	13.9	50.07520025	68
Rudder	2.3	11	14.66562266	42.36
Elevator	2.375	20	15.63767067	42.36

I. Shading/Downwash

To help minimize the effect of downwash, winglets were added to the wing tips [12,13]. By adding winglets, we reduce the induced drag that was created by the vortices. This results in more efficiency that helps with carrying payload and minimizing the power needed to fly the plane. Figure 13 shows that streamlines from the wing do not interfere with the tail meaning that the tail is able to fly through undisturbed air.

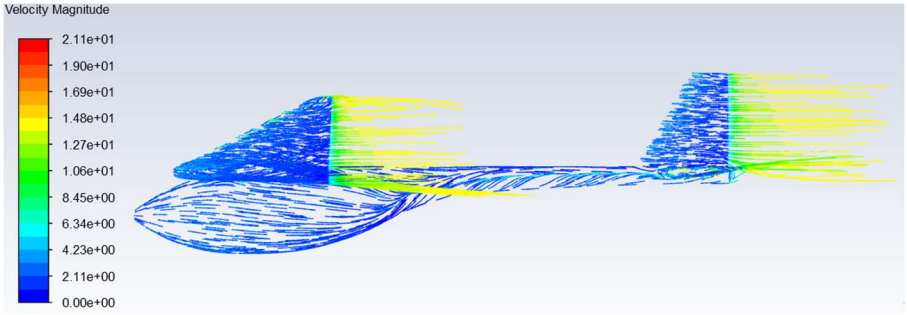

Fig. 13 3D Plane streamlines pattern obtained using ANSYS-Fluent CFD analysis.

J. Dynamic & Static Stability

As per the rules, the plane needs to be able to fly with and without payload. Flying empty, the plane is stable at a 3.469° angle of attack that corresponds to a coefficient of lift of 1.349. Flying with the payload, the plane is stable at a 2.69° angle of attack that corresponds to a coefficient of lift of 1.281. Figure 14 illustrates the pitching moment (coefficient of moment Cm) versus the angle of attack and the coefficient of lift versus the angle of attack, respectively, for both settings.

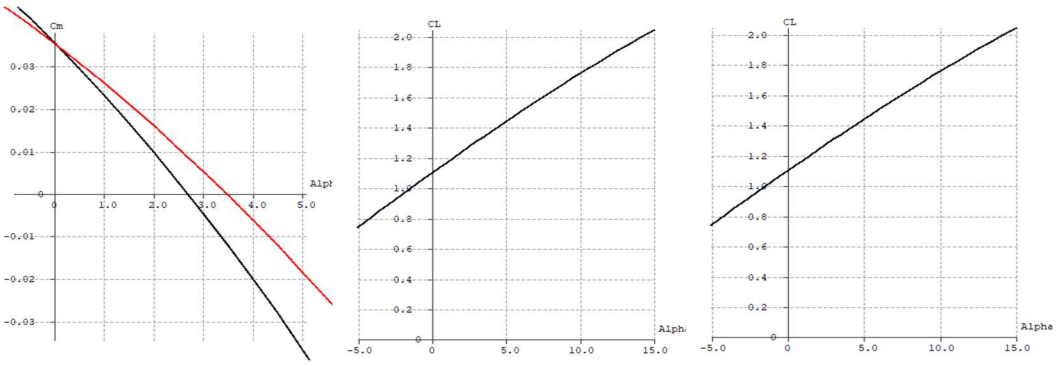

Fig 14. Cm vs AOA & CL vs AOA for the complete 3D airplane (red = empty; black = gross).

We studied the plane's behavior and determined its stability using XFLR5 software as shown before. The root locus graphs were a key to elucidate visually the frequency and damping of each mode to help understand the longitudinal and lateral stability of the plane. As shown in Table 3, the negative values under longitudinal and lateral for modes 1 through 4, except for lateral mode 4, confirm the stability of the plane. The lateral mode 4, which is the spiral mode, is shown to be not stable.

Table 3 Longitudinal and lateral eigenvectors

Mode	Longitudinal	Lateral
1	-5.0319 – 6.1867i	-11.8705
2	-5.0319 + 6.1867i	-2.8798 – 6.5245i
3	-0.0372 – 0.7604i	-2.8798 + 6.5245i
4	-0.0372 + 0.7604i	0.4428

Figure 15 demonstrates the time response of the longitudinal short period and phugoid modes and the lateral roll damping, Dutch roll, and spiral modes. The longitudinal short period mode has a natural frequency of 0.121 Hz and a damping factor of 0.121, while the phugoid mode has a natural frequency of 1.269 Hz and a damping factor of 0.985. The lateral roll damping has a time constant of 0.058 seconds. The Dutch roll mode has a natural frequency of 1.135 Hz and a damping factor of 1.038. Finally, the spiral mode has a time constant of 1.565 seconds.

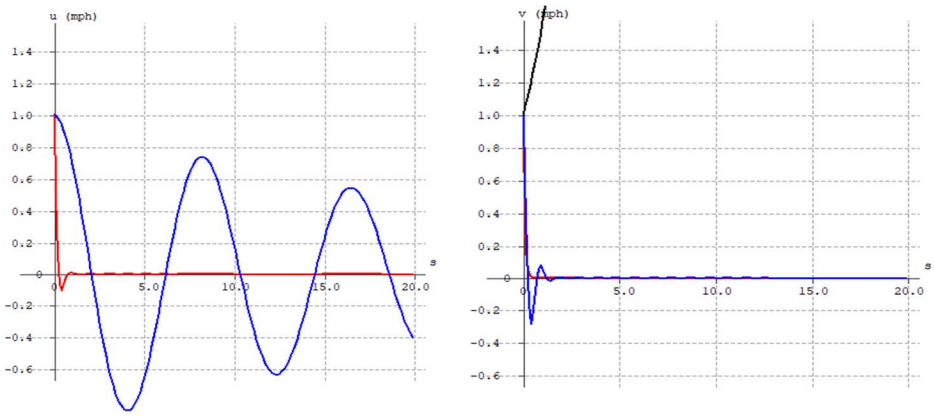

Fig. 15 Phugoid/ short & roll damping/ Dutch roll/ spiral.

K. Aeroelasticity

After completing the structural analysis of the wing, we noticed that the wing would experience significant deflections of 1.612 inches. As a result, we decided to redo the stability analysis, by adding a dihedral of 2 inches to the wing. The results show that even with the dihedral on the wing, the plane is still longitudinally and laterally stable as shown in Fig. 16. As shown without the dihedral, the phugoid, short, roll damping, and Dutch roll responses remain stable unlike the spiral.

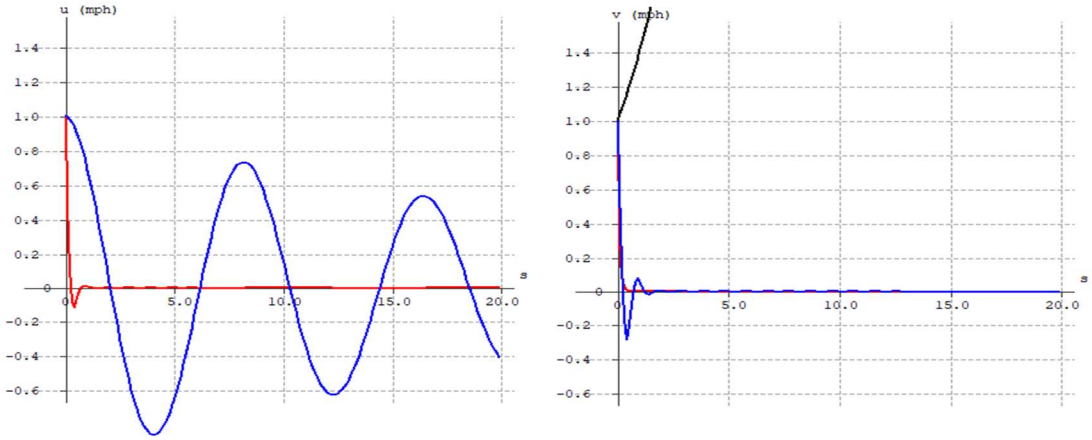

Fig. 16 Phugoid/ short & roll damping/ Dutch roll/ spiral with wing dihedral included.

L. Lifting Performance, Payload Prediction, and Margin

The steel plates were located surrounding the soccer ball to prevent the cargo length from increasing past the diameter of a soccer ball. Steel was evenly distributed in front and behind the soccer ball to maintain the balance of the plane, while the battery was positioned behind the payload to balance the plane. With the plane balanced, 27.5 lbf of lift are needed to take off and about 30 lbf of lift are needed to consider the plane turning in a bank. When the plane has no cargo, it has a stability margin of 5.449%.

VI. Conclusion

The PAC-5 is a 6.54-lb regular class aircraft designed to carry 20 lbf of payload in the form of steel plates and one soccer ball. It was designed subject to a constrained wingspan, while having easy access to the payload *via* the detachable nose of the plane. A true multi-disciplinary analysis and a multi-objective optimization of five geometric parameters for aerodynamic performance were conducted using state-of-the-art collection of software and a parallel computer. Many of the design decisions and optimizations for this aircraft were made based on information gathered from various programs we used, researching the internet, and learning from our faculty advisor who guided us at every stage. The resulting Pareto-optimum 3D airplane geometry provided a 5.03% increase in lift, a 9.75% decrease in drag, and a 40.88% decrease in the pitching moment, while providing good structural integrity and flight stability

Acknowledgments

The first two authors are grateful for the advices and guidelines of the faculty member of this team project, Prof. George S. Dulikravich. They are also expressing their gratitude to two graduate students, Janhavi Chitale and Ann-Kayanna Blanchard, in Prof. Dulikravich's MAIDROC Laboratory for teaching them how to run various software and how to use a parallel computer. Sincere thanks are also due Dr. Helmut Sobieczky for providing his versatile shape generation software and instructions on how to use it.

References

[1] Cobra. Cobra Motors. (Retrieved from https://www.cobramotorsusa.com/motors-4130-20.html on Nov. 25, 2020)
[2] RimFire. RimFire Outrunner Brushless Motors. (Retrieved from GreatPlanes.com: http://greatplanes.com/motors/gpmg4505.php on January 2, 2021)
[3] UnderGround Weather. Lakeland, Florida Weather History. (Retrieved from Underground.com: https://www.wunderground.com/history/daily/us/fl/tampa/KTPA/date/2015-3-8 on January 15, 2020)
[4] Nicolai, L. M., and Vural, M., *Estimating R/C Model Aerodynamics and Performance*. Illinois Institute of Technology, Chicago, IL, USA, 2020.
[5] Raymer, D. P., *Aircraft Design: A Conceptual Approach*. American Institute of Aeronautics and Astronautics, Washington, DC, USA, 1992
[6] Sobol, I.M., "Distribution of points in a cube and approximate evaluation of integrals," *U.S.S.R Comput. Maths. Math. Phys,* 7, 1967, pp. 86-112.
[7] ANSYS Fluent http://ansys.com/Products/Simulation+Technology/Fluid+Dynamics
[8] modeFRONTIER, Software Package, Ver. 4.5.4, ESTECO, Trieste, Italy.
[9] Scott, J., Aircraft Landing Gear Layouts. (Retrieved from aerospaceweb.org: http://www.aerospaceweb.org/question/design/q0200.shtml on Oct. 31, 2020).
[10] Sobieczky, H., E300 Geometry Generation Code, Vienna, Austria, 2020.
[11] Sobieczky, H. "Geometry generator for CFD and applied aerodynamics", *New Design Concepts for High Speed Air Transport,* CISM Courses and Lectures No. 366, Springer, Wien, New York, 1997, pp. 137-157.
[12] Reddy, S. R., Sobieczky, H., Abdoli, A., and Dulikravich, G. S., "Multi-Winglets: Multiobjective Optimization of Aerodynamic Shapes", *AIAA Journal of Aircraft,* Vol. 53, No. 4, July 2016, pp. 992-1000.
[13] National Aeronautics and Space Advisory (NASA). Downwash Effects on Lift. (Retrieved from NASA.gov: https://www.grc.nasa.gov/www/k-12/airplane/downwash.html on January 14, 2020)